arXiv:hep-ph/0012316v1 22 Dec 2000

December, 2000
hep-ph/0012316

On Radiative Weak Annihilation Decays

Richard F. Lebed*

Department of Physics and Astronomy
Arizona State University, Tempe, AZ 85287 USA

We discuss a little-studied class of weak decay modes sensitive to only one quark topology at leading order in G_F: $M \to m\gamma$, where M, m are mesons with completely distinct flavor quantum numbers. Specifically, they proceed via the annihilation of the valence quarks through a W and the emission of a single hard photon, and thus provide a clear separation between CKM and strong interaction physics. We survey relevant calculations performed to date, discuss experimental discovery potential, and indicate interesting future directions.

Presented at the

5th International Symposium on Radiative Corrections
(RADCOR–2000)
Carmel CA, USA, 11–15 September, 2000

*Work supported by the Department of Energy under Grant No. DE-AC05-84ER40150.

The feature that makes heavy quark physics appealing—the decoupling of the heavy quark matrix elements from those of the light degrees of freedom—can prove to be treacherous if one cannot track the processes through which the quarks of various flavors are created or destroyed. Such ambiguities plague the extraction of Cabibbo-Kobayashi-Maskawa (CKM) elements from nonleptonic weak decays.

In this light, processes with unusual flavor quantum numbers are useful since they serve to distinguish the weak interaction and strong interaction physics: As seen below, unusual flavor quantum numbers imply a very limited number of possible Feynman diagram topologies. The price one must pay for this clarity is that such interesting decays tend to be quite rare. In particular, the modes $M \to m\gamma$ discussed in this talk are radiative (rates $\propto \alpha_{\rm EM}$) weak ($\propto G_F^2 |V^* V|^2$) processes with pointlike annihilation ($\propto f_M/M \cdot f_m/m$, where f indicates the meson decay constant). Nevertheless, we argue below that once such modes are produced, they should be relatively easy to detect.

To study the flow of flavor in a flavor-changing weak decay process, it is sufficient to work at the partonic level with simple quark diagrams, since gluons and sea quark pairs carry only flavor-singlet quantum numbers. Only valence quarks and vacuum-produced $q\overline{q}$ pairs that become valence quarks need be considered. Thus, the complications of QCD are irrelevant if one wishes only to classify weak decay processes. As shown in Ref. [1], only six such classes exist at $O(G_F^1)$, since only the W boson changes flavors in the standard model. These classes are T (color-unsuppressed tree), C (color-suppressed tree), P (penguin), A (weak annihilation), E (weak exchange), and PA (penguin annihilation) diagrams, as depicted in Fig. 1.

One may now enumerate a number of problems inherent to computing weak meson decays of the form $M \to m_1 m_2$. The first such difficulty is the most obvious and endemic to any hadronic process, namely, that hadron wavefunctions are not precisely known and must be modeled in order for a calculation to be performed. Second, for electrically neutral mesons—even with valence quarks with distinct flavors—the asymptotic states are not pure flavor eigenstates, and then one must take into account $K\overline{K}$, $D\overline{D}$, $B\overline{B}$, or $B_s\overline{B}_s$ mixing.

In addition, however, there are complications best seen by using the diagrammatic classification. While it is true that any arbitrarily complicated Feynman diagram for a flavor-changing $M \to m_1 m_2$ meson decay falls uniquely into one of these six classes, it is also true that any such decay tends to have contributions from more than one topology. In particular, processes that have a T diagram often also have a C diagram, and the two can mix under final-state interactions (FSI's). As an example, consider $B^+ \to \pi^+ \overline{D}^0 = \overline{b}u \to (u\overline{d})(\overline{c}u)$. The weak decay at the quark level may proceed through $\overline{b} \to \overline{c} W^+ \to \overline{c} u \overline{d}$, and the u valence quark in π^+ may either come from the weak vertex or the spectator. In other cases, valence quarks may emerge from pair creation due to fragmentation. The basic problem here is one of redundant quark flavor in the final state: Since two u quarks are indistinguishable, one is faced with

the problem of where each one originates, and this redundancy is forced by the limited number of distinct quark flavors available for hadron formation.

Another affliction of $M \to m_1 m_2$ best seen in terms of the diagram topologies is the problem of "generalized penguin pollution," which we define to be the contribution to a decay from at least two diagrams containing different CKM couplings. A classic example is the decay $B^0 \to \pi^+\pi^- = \overline{b}d \to (u\overline{d})(d\overline{u})$. In the T diagram, the weak decay at the quark level is $\overline{b} \to \overline{u}W^+ \to \overline{u}u\overline{d}$, where the $\overline{u}$ quark hadronizes with

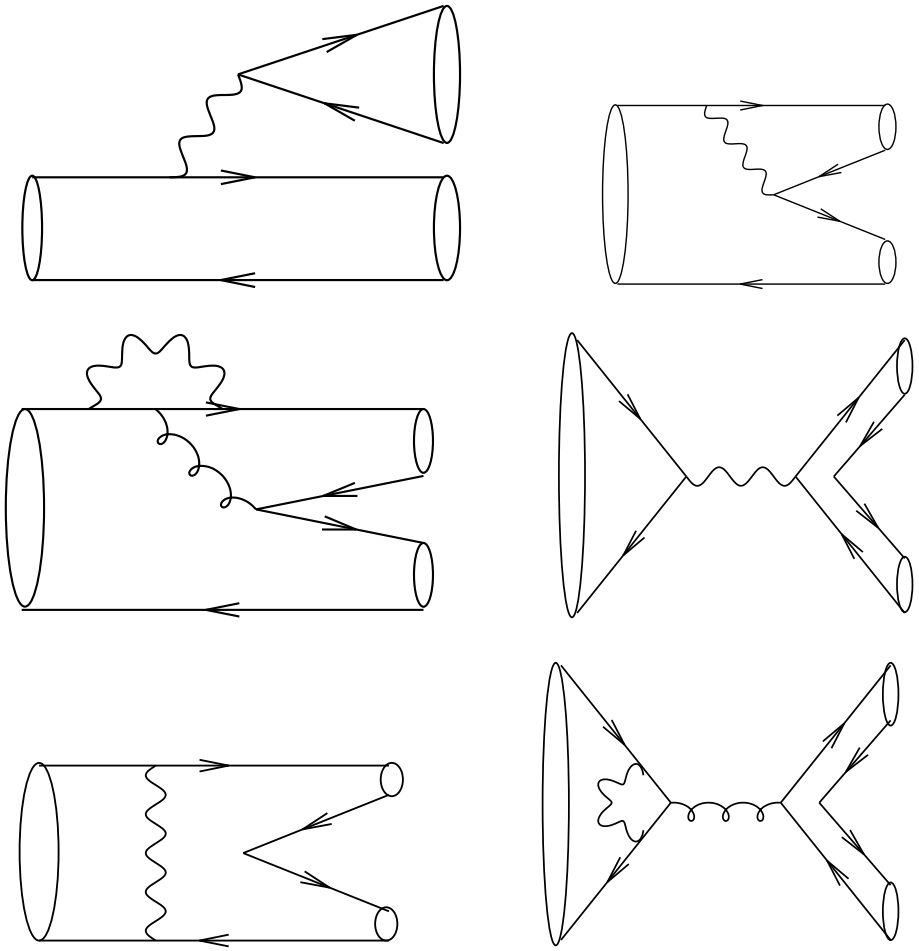

Figure 1: The six flavor-changing weak decay topologies at $O(G_F^1)$. Reading across and from top to bottom, these are labeled T, C, P, A, E, and PA, respectively. Ovals indicate hadronization into color-singlet mesons. For processes with the T topology, there is often also a C diagram contribution, so that the two classes can mix through final-state interactions. The P, A, E, and PA diagrams have variants in which the the $q\overline{q}$ pair from the vacuum hadronize into a single flavor-singlet meson.

the spectator d quark, and the CKM coefficient is $V_{ub}^* V_{ud}$. On the other hand, a P diagram may also contribute (hence the original name "penguin pollution"), in which $\overline{b} \to \overline{d} g \to \overline{d} u \overline{u}$. The penguin loop, dominated by the top quark contribution, produces primarily the CKM coupling $V_{tb}^* V_{td}$. Again, the ultimate reason that a large proportion of possible modes exhibit generalized penguin pollution is the existence of a limited number of quark flavors available for the decay: In the example, the $u\overline{u}$ pair can either emerge from a strong or weak process.

Typically, $M \to m_1 m_2$ meson decays tend to suffer at least one of the latter two problems. It is difficult to find modes proceeding through only one topology, chiefly owing to the limited number of distinct quark flavors; in particular, $M \to m_1 m_2$ contains six quarks, while only the lightest five quark flavors form mesons.

To evade this problem, let us consider instead the meson decays $M \to m\gamma$ [2]. Here one has only four quarks, which can easily be chosen distinct. In this case there is clearly (as a few moments' study of Fig. 1 should convince the reader) only one weak topology available at $O(G_F^1)$: If the meson is charged, then $M^+ \to m^+ \gamma$ proceeds uniquely through the weak annihilation (A) diagram, while if the meson is neutral, then $M^0 \to m^0 \gamma$ proceeds uniquely through the weak exchange (E) diagram. To date, no such decays have been observed, so an order-of-magnitude calculation of their rates serves to guide not only future calculations, but experimental searches as well. The photon may be attached to any charged particle line, and is hard and monochromatic, fixed in energy due to the restrictive kinematics of two-body decays. The E processes are certainly interesting, but introduce the problem of $M^0 \overline{M}^0$ and $m^0 \overline{m}^0$ mixing mentioned above, so we concentrate below on the A processes.

Thus far we have considered contributions only at $O(G_F^1)$. One may also neglect the diagram in which the photon couples to the $W^\pm$, since it produces an extra $1/M_W^2$ propagator suppression; thus, one need consider only diagrams in which the photon couples to one of the quarks. At a similar numerical size for A processes are the $O(G_F^2)$ diagrams depicted in Fig. 2. These consist of "di-penguin" and crossed-box diagrams; however, neither class is expected to be particularly large, since the enhanced significance of ordinary penguin and box diagrams occurs due to virtual t quark lines in the loops. In the case of charged mesons, one of the valence quarks is necessarily u-type, and the virtual quark connecting to it through a W vertex is necessarily d-type, and thus does not give rise to a large contribution. One concludes that, in the standard model at least, the $O(G_F^1)$ contribution should dominate the rate for A processes.

This begs the question of whether any common non-standard physics might contribute to, or even dominate, A processes. Two very simple possibilities jump immediately to mind. First, the s-channel exchange of a W may be replaced with the t-channel exchange of a flavor-changing neutral current (FCNC) boson X. Such a

process is important if

$$\frac{V_1 V_2}{M_W^2} \lesssim \frac{g_1 g_2}{M_X^2}, \tag{1}$$

where V_i and g_i represent the CKM and new physics couplings, respectively, at the two vertices. The best potential for new physics discovery is when g_i are $O(1)$ and V_i are as small as possible. For example, in the case $B^+ \to D^{*+}\gamma$, $V_1 = V_{ub}^* \sim \lambda^3$ and $V_2 = V_{cd} \approx \lambda$, with Wolfenstein $\lambda \approx 0.2$. Then one immediately finds

$$M_X \lesssim 2 \text{ TeV}, \tag{2}$$

a fairly stringent bound, considering that one must still make sure that $K\overline{K}$ mixing and other FCNC constraints are properly taken into account.

Another possibility is the s-channel exchange of a charged Higgs boson. Since the current lower limit [3] is $M_{H^+} > 130$ GeV, these decays are a possible place to find new physics (using the same tree-level estimation as above) if the corresponding $H^+ q\overline{q}$ Yukawa couplings are not smaller than the CKM elements $V_1 V_2$.

Having discussed the restrictive nature of flavor distinctiveness on generating processes with unique flavor topologies, it is natural to present the complete list [2] of such decays for pure A processes. One must choose two from the list $\{b, s, d\}$ and two from the list $\{c, u\}$, for a total of six possibilities. Only the lightest pseudoscalar M of each flavor content decays dominantly weakly. Then angular momentum conservation requires that the spin of the photon must be balanced by a daughter meson m of spin ≥ 1; for sake of illustration, we take m to be the lowest-lying vector meson, which should presumably boast the largest transition rate for any state with the given final flavor quantum numbers. Table 1 presents the modes just described, along with the corresponding CKM coefficients.

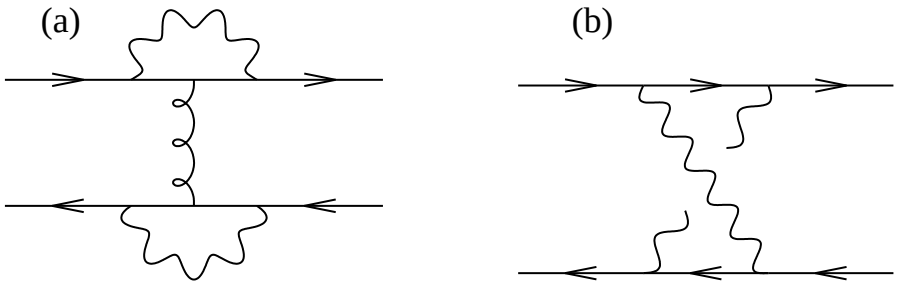

Figure 2: Diagrams contributing at $O(G_F^2)$ to processes described at $O(G_F^1)$ by the A diagram of Fig. 1. These are the (a) "di-penguin" and (b) crossed-box diagrams. The gluons emerging from the W loops in the di-penguin need not be the same; indeed, the two penguins can be separated by long-distance effects.

Table 1: Flavor structure and mesonic decay modes of weak annihilation radiative decays. The CKM coefficient for each process is accompanied by its magnitude in powers of Wolfenstein $\lambda \approx 0.2$.

Valence structure	Decay mode	CKM Elements
$\overline{b}u \to c\overline{s}\gamma$	$B^+ \to D_s^{*+}\gamma$	$V_{ub}^* V_{cs} \sim \lambda^3$
$\overline{b}u \to c\overline{d}\gamma$	$B^+ \to D^{*+}\gamma$	$V_{ub}^* V_{cd} \sim \lambda^4$
$\overline{b}c \to u\overline{s}\gamma$	$B_c^+ \to K^{*+}\gamma$	$V_{cb}^* V_{us} \sim \lambda^3$
$\overline{b}c \to d\overline{u}\gamma$	$B_c^+ \to \rho^+\gamma$	$V_{cb}^* V_{ud} \sim \lambda^2$
$c\overline{d} \to u\overline{s}\gamma$	$D^+ \to K^{*+}\gamma$	$V_{cd}^* V_{us} \sim \lambda^2$
$c\overline{s} \to u\overline{d}\gamma$	$D_s^+ \to \rho^+\gamma$	$V_{cs}^* V_{ud} \sim \lambda^0$

Note that the CKM suppression of the decays varies widely, from none in the case of $D_s^+ \to \rho^+\gamma$ to λ^4 in the case of $B^+ \to D^{*+}\gamma$. These decays appear to have been discussed only rarely in the literature. $D_s^+ \to \rho^+\gamma$ has been considered using the quark model [4], pole and vector meson dominance methods [5], light-cone techniques [6], and effective field theory [7]. The double Cabibbo-suppressed mode $D^+ \to K^{*+}\gamma$, interesting since it is a neutrinoless decay sensitive to $|V_{cs}|$, was also considered in Refs. [5,7]. The modes $B^+ \to D_s^{*+}\gamma$ and $D^{*+}\gamma$ (collectively, $D_{(s)}^{*+}\gamma$) were first considered in Ref. [8], where they were suggested as possible probes of $|V_{ub}|$. The modes $B_c \to \rho^+\gamma$ and $K^{*+}\gamma$ were first considered [9] in the context of light-cone sum rules.

Let us consider in further detail the calculation of Ref. [8] since its methods and approximations figure large in the rest of this talk. In [8], heavy quark effective theory (HQET) and light-quark SU(3) are used to relate the four-fermion vertex $(\overline{b}u)(c\overline{d})$ or $(\overline{b}u)(c\overline{s})$ appearing in the decays $B^+ \to D_{(s)}^{*+}\gamma$ to the vertex $(\overline{b}d)(b\overline{d})$ that appears in $B\overline{B}$ mixing. Such an approach of course neglects the "bag parameter" B (*i.e.*, the multiplicative long-distance correction to factorization) relevant to each vertex, as well as the mixing and short-distance renormalization of the two different color Fierz orderings of the four-fermion operator.

The next problem is how to incorporate long-distance effects between the weak and electromagnetic vertices. Here, the simplest ansatz is adopted: One assumes that only the lightest meson propagates between the two vertices with the same flavor quantum numbers as the meson on the other side of the photon vertex, and the same spin-parity as the meson on the other side of the weak vertex, . This is depicted in Fig. 3. In each diagram the external states are B^+ and $D_{(s)}^{*+}$, while in the first the intermediate meson is B^{*+}, and in the second it is $D_{(s)}^+$. This approximation not only neglects all higher resonances that may contribute in the intermediate state (for example,

$D_{(s)}(2S)$), but also vector-dominance diagrams in which the photon is generated by a resonance of a valence quark from one of the mesons and an antiquark from the weak vertex (such as $B^+ \to D_s^{*+}\rho^0 \to D_s^{*+}\gamma$), and multiparticle intermediates (such as $B^+ \to D^0 K^+ \to D_s^{*+}\gamma$) in which FSI's play an important role.

Finally, HQET is used to relate the $BB^*\gamma$ and $D_{(s)}D^*_{(s)}\gamma$ couplings to $\Gamma(D^{*+} \to D^+\gamma)$, for which an experimental upper bound exists [3]. One finds the branching ratios (BR's)

$$\begin{aligned}
&\mathrm{BR}(B^+ \to D_s^{*+}\gamma) \\
&\quad = \; 2\times 10^{-7}\left(\frac{B_B}{0.98}\right)^2 \left|\frac{V_{ub}^* V_{cs}}{3\times 10^{-3}}\right| \left(\frac{\Gamma(D^{*+})}{0.131\,\mathrm{MeV}}\right)\left(\frac{\mathrm{BR}(D^{*+}\to D^+\gamma)}{3.2\%}\right), \\
&\mathrm{BR}(B^+ \to D^{*+}\gamma) \\
&\quad = \; 7\times 10^{-9}\left(\frac{B_B}{0.98}\right)^2 \left|\frac{V_{ub}^* V_{cd}}{6.6\times 10^{-4}}\right| \left(\frac{\Gamma(D^{*+})}{0.131\,\mathrm{MeV}}\right)\left(\frac{\mathrm{BR}(D^{*+}\to D^+\gamma)}{3.2\%}\right).
\end{aligned} \tag{3}$$

The final approximation, using an on-shell electromagnetic coupling (the $D^{*+} \to D^+\gamma$ transition magnetic moment) to extract the coupling of an intermediate meson, off-shell by the large amount $m^2(B^+) - m^2(D^+_{(s)})$ in the second diagram (as fixed by the fact that the real photon has $q^2 = 0$), deserves special comment. In the original calculation [8], a new formal heavy quark limit $m_b - m_c \lesssim \Lambda_{\mathrm{QCD}} \ll m_{c,b}$ was invented, for which the virtuality of the electromagnetic coupling is parametrically small. It is of course possible to remove this assumption when the photon is virtual, as in $B^+ \to D^{*+}_{(s)}e^+e^-$; then one may find a kinematic region where the intermediate meson is approximately at rest [10], or do even better and develop an operator product expansion (OPE) in the variable $q^2 \gg \Lambda^2_{\mathrm{QCD}}$. Then one calculates [11], for example,

$$\mathrm{BR}(B^+ \to D_s^{*+}e^+e^-)\Big|_{q^2>1\,\mathrm{GeV}^2} \approx 1.8\times 10^{-9}. \tag{4}$$

The authors of Refs. [10,11] also tackle the problem of radiative weak exchange (the E rather than A diagram) exclusive processes using the OPE approach in Ref. [12],

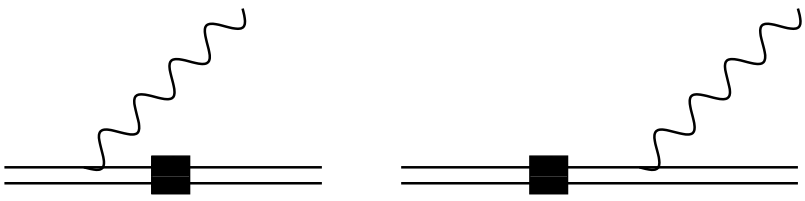

Figure 3: Diagrams for $B^+ \to D^{*+}_{(s)}$, assuming dominance of long-distance physics by single-meson states. The square indicates the weak interaction vertex.

Table 2: Estimates of branching ratios for weak annihilation decays using Eq. (5). Also included are energies of the monochromatic photon.

Decay mode	BR (est.)	Photon Energy (GeV)
$B^+ \to D_s^{*+}\gamma$	1×10^{-7}	2.22
$B^+ \to D^{*+}\gamma$	7×10^{-9}	2.26
$B_c^+ \to K^{*+}\gamma$	3×10^{-6}	3.14
$B_c^+ \to \rho^+\gamma$	3×10^{-5}	3.15
$D^+ \to K^{*+}\gamma$	6×10^{-7}	0.72
$D_s^+ \to \rho^+\gamma$	8×10^{-5}	0.83

finding similar branching ratios. The much smaller rates for e^+e^- processes compared to those for on-shell photon processes of course arise from the additional factor of $\alpha_{\rm EM}$ from conversion of the virtual photon.

One may also consider a simultaneous calculation [2] of all of the decays in Table 1 by using an approach similar to that of Ref. [8] but dropping the heavy quark approximations. In this case, let us consider only the second diagram of Fig. 3, where the photon couples only to the lighter vector meson V, and denote the initial and intermediate pseudoscalar mesons as M and P, respectively. We restrict to this single diagram because no positive measurements of $MM^*\gamma$ couplings have yet appeared (recall that we used an upper bound for $DD^*\gamma$), while $\Gamma(K^{*+} \to K^+\gamma)$ and $\Gamma(\rho^+ \to \pi^+\gamma)$ are known. This simple calculation yields

$$\begin{aligned}\Gamma(M \to V\gamma) &= \frac{3}{2} G_F^2 \left|V_M V_P\right|^2 f_M^2 f_P^2 B^2 \, \Gamma_{V\to P\gamma} \left[\frac{\mathcal{C}(M^2 - m_P^2)}{\mathcal{C}(0)}\right]^2 \\ &\quad \times \left(\frac{M^2}{M^2 - m_P^2}\right)^2 \left(\frac{M^2 - m_V^2}{m_V^2 - m_P^2}\right)^3 \left(\frac{m_V}{M}\right)^3 , \end{aligned} \tag{5}$$

where B is the relevant bag parameter, the width $\Gamma_{V\to P\gamma} \propto \alpha_{\rm EM}$, and the off-shell extrapolation of the electromagnetic form factor, labeled $\mathcal{C}$, is explicitly indicated. Values for branching ratios for the six modes, along with the photon energies, are listed in Table 2.

We see that the Cabibbo-unsuppressed decay $D_s^+ \to \rho^+\gamma$ has a rate already large enough that it might already have been produced at Fermilab or CLEO. Certainly it will be produced copiously at BABAR and BELLE, where also the rarer B^+ modes may be observed in smaller but still significant numbers. The B_c channels must necessarily wait for hadron machines such as LHC or BTeV.

One may also consider information contained in the helicity of the photon. For

an arbitrary $P(0^-) \to V(1^-)\gamma$ decay, the generic amplitude is

$$\mathcal{M} = \epsilon_\mu^{*(V)} \epsilon_\nu^{*(\gamma)} \left[i\mathcal{A}_{PC}\, \epsilon^{\mu\nu\rho\sigma} p_\rho^{(V)} p_\sigma^{(P)} + \mathcal{A}_{PV} \left(p^{(P)\,\mu} p^{(P)\,\nu} - g^{\mu\nu}\, p^{(\gamma)} \cdot p^{(P)} \right) \right], \qquad (6)$$

where PC, PV distinguish parity conserving and violating amplitudes, respectively. Then the total rate is

$$\begin{aligned} \Gamma &= \frac{1}{8\pi} |\mathbf{p}|^3 \left(|\mathcal{A}_{PC} + \mathcal{A}_{PV}|^2 + |\mathcal{A}_{PC} - \mathcal{A}_{PV}|^2 \right) \\ &= \frac{1}{4\pi} |\mathbf{p}|^3 \left(|\mathcal{A}_{PC}|^2 + |\mathcal{A}_{PV}|^2 \right), \end{aligned} \qquad (7)$$

where $|\mathbf{p}| = (m_P^2 - m_V^2)/2m_P$. The first line of Eq. (7) is separated into contributions in which the two vector particles are both right-handed (RR) and left-handed (LL) , respectively. Indeed, the asymmetry is

$$\frac{\Gamma_{RR} - \Gamma_{LL}}{\Gamma} = \frac{2\mathrm{Re}\, \mathcal{A}_{PC} \mathcal{A}_{PV}^*}{|\mathcal{A}_{PC}|^2 + |\mathcal{A}_{PV}|^2} \ . \qquad (8)$$

The relative weights of the two helicities may prove to be especially interesting since the $V-A$ nature of weak interactions weights the two photon helicities differently. For example, in the case of penguin $B^- \to K^{*-}\gamma$ and $\rho^-\gamma$ decays, the L helicity has been found [13] to be enhanced compared to R. This enhancement persists [14] even when long-distance corrections (including contributions from A diagrams) are included. Certainly, a measured enhancement of the disfavored helicity would be a signal of new physics. Studies of the role of photon helicities are also underway [15] in the pure A decays described here.

The radiative weak annihilation decays occupy a unique position in heavy flavor physics, in that they are completely flavor self-tagged and kinematically trivial. Their experimental observation is imminent and promises another handle on the CKM matrix. Once the most common mode $D_s^{*+} \to \rho^+\gamma$ is observed, its measured branching ratio may be used to study the other decays. Alternately, lattice simulations may be used to probe the generalized bag parameters, one may relate nonleptonic A processes to semileptonic radiative modes such as $B \to \gamma\ell\nu$ [14,16], or one may consider alternate new physics contributions. On both the theoretical and experimental fronts, many opportunities for advances exist.

Acknowledgments

I thank the University of Maryland Theoretical Quarks, Hadrons, and Nuclei group for their hospitality.

References

[1] M. Gronau, O.F. Hernandez, D. London, and J.L. Rosner, *Phys. Rev.* **D50** (1994) 4529.

[2] R.F. Lebed, *Phys. Rev.* **D61** (2000) 033004.

[3] D.E. Groom *et al.* (Particle Data Group), *Eur. Phys. J.* **C15** (2000) 1.

[4] P. Asthana and A.N. Kamal, *Phys. Rev.* **D43** (1991) 278.

[5] G. Burdman, E. Golowich, J.L. Hewett, and S. Pakvasa, *Phys. Rev.* **D52** (1995) 6383.

[6] A. Khodjamirian, G. Stoll, and D. Wyler, *Phys. Lett.* **B358** (1995) 129.

[7] S. Fajfer, S. Prelovšek, and P. Singer, *Eur. Phys. J.* **C6** (1999) 471; S. Fajfer and P. Singer, *Phys. Rev.* **D56** (1997) 4302; B. Bajc, S. Fajfer, and R.J. Oakes, *ibid.* **51** (1995) 2230.

[8] B. Grinstein and R.F. Lebed, *Phys. Rev.* **D60** (1999) 031302(R).

[9] T.M. Aliev and M. Savci, *J. Phys.* **G24** (1998) 2223.

[10] D.H. Evans, B. Grinstein, and D.R. Nolte, *Phys. Rev.* **D60** (1999) 057301.

[11] D.H. Evans, B. Grinstein, and D.R. Nolte, *Phys. Rev. Lett.* **83** (1999) 4947.

[12] D.H. Evans, B. Grinstein, and D.R. Nolte, *Nucl. Phys.* **B577** (2000) 240.

[13] Y. Grossman and D. Pirjol, *JHEP* **0006** (2000) 029.

[14] B. Grinstein and D. Pirjol, *Phys. Rev.* **D62** (2000) 093002.

[15] C.E. Carlson, R.F. Lebed, and A. Petrov, in preparation.

[16] G.P. Korchemsky, D. Pirjol, and T.-M. Yan, *Phys. Rev.* **D61** (2000) 114510.